

Preparation Technologies and Electrochemical Properties of Hydrogen Storage Alloys



Zhang Yanghuan

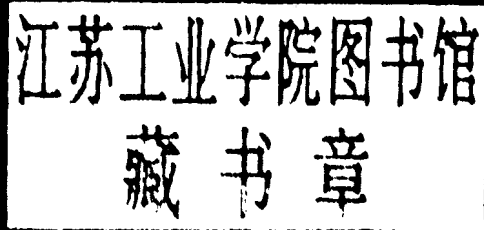
Wang Xinlin

Metallurgical Industry Press

Preparation Technologies and Electrochemical Properties of Hydrogen Storage Alloys



Zhang Yanghuan
Wang Xinlin



METALLURGICAL INDUSTRY PRESS

Copyright © 2008 by Metallurgical Industry Press, China
Published and Distributed by
Metallurgical Industry Press
39 Songzhuyuan North Alley, Beiheyuan St.
Beijing 100009, P. R. China

All rights reserved. No part of this publication may be reproduced, stored in a retrieval system, or transmitted in any form or by any means, electronic, mechanical, photocopying, recording or otherwise, without the prior written permission of the copyright owner.

图书在版编目(CIP)数据

贮氢合金的制备技术和电化学性能/张羊换,王新林著.
—北京:冶金工业出版社,2008.3
ISBN 978-7-5024-4443-3

I. 贮… II. ①张… ②王… III. ①贮氢合金-制备
②贮氢合金-电化学 IV. TG139-53

中国版本图书馆 CIP 数据核字 (2008) 第 006542 号

出 版 人 曹胜利

地 址 北京北河沿大街嵩祝院北巷 39 号,邮编 100009

电 话 (010)64027926 电子信箱 postmaster@cnmip.com.cn

责任编辑 郭冬艳 程志宏 美术编辑 李 心 版式设计 张 青

责任校对 侯 璐 责任印制 丁小晶

ISBN 978-7-5024-4443-3

北京百善印刷厂印刷;冶金工业出版社发行;各地新华书店经销

2008 年 3 月第 1 版,2008 年 3 月第 1 次印刷

210mm×297mm;17 印张;748 千字;261 页;1—800 册

85.00 元

冶金工业出版社发行部 电话:(010) 64044283 传真:(010) 64027893

冶金书店 地址:北京东四西大街 46 号(100711) 电话:(010) 65289081

(本书如有印装质量问题,本社发行部负责退换)

序

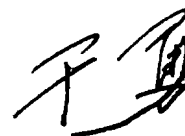
贮氢合金问世可追溯到 20 世纪 60 年代中期。或许是第二次中东战争引发石油危机的缘故，各国科学家们急于寻求新的替代能源，贮氢材料的研究受到普遍重视。1964 年美国布鲁克—海文国家实验室合成了 Mg_2Ni 合金，贮氢量（质量分数）3.6%，常压下 250℃ 能析出氢，可谓是历史上最早的贮氢合金。1968 年荷兰飞利浦实验室在研究永磁材料 SmCo_5 时意外地发现了稀土贮氢合金。1970 年荷兰 Philips 发现 LaNi_5 合金，在稀土贮氢合金中，具有最为理想的贮氢性能，贮氢量（质量分数）1.4%。

将 LaNi_5 型贮氢合金作为二次电池负极材料的研究始自 1973 年。1984 年研究解决了 LaNi_5 合金在充放电过程中容量衰减迅速的问题，从而实现了利用贮氢合金作为负极材料制造 Ni-MH 电池的可能。美国在 1987 年建成 Ni-MH 电池试生产线，日本 1989 年进行了 Ni-MH 电池试生产。我国在 1990 年利用国产的原材料和自己开发的工艺技术，研制出我国第一只“AA”型 Ni-MH 电池，并在国家“863”计划的支持下，于 1992 年在广东省中山市建立了国家高技术新型储能材料工程开发中心和 Ni-MH 电池试生产基地，有力地推动了我国贮氢材料和 Ni-MH 电池的研制及其产业化进程。目前，我国已是世界上稀土基 AB_5 型贮氢材料和 Ni-MH 电池产销量的第一大国。

随着贮氢材料应用领域的不断拓宽，对贮氢材料的性能要求越来越高，促使研究不断深入，力图发现容量更高、寿命更长、价格低廉的新型贮氢材料。特别是近年来，贮氢合金研究呈现新的趋势，不仅注重合金的成分设计，而且将特种工艺，比如真空快淬、机械合金化等一些新的材料制备技术应用到贮氢材料的制备中，取得了显著的效果。钢铁研究总院从 20 世纪 80 年代初开始贮氢合金的研究工作，并在全国率先将真空快淬技术应用到各种贮氢合金的制备中，特别是应用真空快淬技术制备的低成本稀土基 AB_5 型贮氢合金，获得国家“九五”、“十五”、“863 计划”两个项目的支持，一个创新基金项目的支持；用真空快淬工艺制备新型高容量贮氢合金获得国家自然科学基金重点项目和面上项目的支持，取得了一系列有重要科学意义和应用价值的研究成果，独具特色，受到国内外同行的关注。在国内外学术期刊

上发表贮氢合金研究专题论文一百余篇，获得国家发明专利多项，为贮氢合金的研究赶超世界先进水平做出了重要贡献。由两位教授编著的《贮氢合金的制备技术及电化学性能》收编了他们近年来在贮氢材料研究领域的一部分论文，集中反映了真空快淬技术在贮氢合金制备中的一些重要成果。特别是易挥发的镁基贮氢材料的冶炼与快淬技术鲜见报道，对于本领域的研究者具有重要的参考价值。相信读者通过阅读《贮氢合金的制备技术及电化学性能》，对真空快淬技术以及快淬贮氢材料的微观结构及电化学性能特点有一个比较深入的了解，获得裨益。本书的出版，将有益于促进贮氢材料领域研究者的深入交流与合作，从而推动我国贮氢材料的研究向更高水平发展。

中国工程院院士



2007年7月10日

前 言

氢能是一种最清洁的可再生能源，具有取之不尽、用之不竭的优势。以石油为主的现代能源系统使社会产生了巨大的能源危机，促使人们研究具有极大的科学价值和社会效益的非碳燃料，同时人类对环境的高度关注，也期待着“绿色能源”的开发和应用，而氢能则最大限度地符合了人类的这种期待。氢是 21 世纪的重要新能源之一，世界各国对氢能的应用予以高度重视。氢的廉价制取、存储与运输则是氢能源开发应用的重点研究课题。

贮氢材料因其能可逆地大量吸收和放出氢气，在氢的储存与输送过程中充当一种重要载体，加之氢与贮氢材料均是“绿色”环保产品，因此备受世界各国的高度重视。

金属氢化物、碳纤维、碳纳米管以及某些有机液体都是优良的贮氢材料，特别是金属氢化物，不仅是一种优良的贮氢材料，而且还是一种新型功能材料，可用于电能、机械能、热能和化学能的转换与储存，具有广泛的应用前景。因此，金属氢化物技术，包括材料开发以及应用技术的研究，近年来受到包括我国在内的世界各国的广泛重视，得到了迅速的发展。我国在“863”高新技术发展规划、“973”计划以及国家自然科学基金指南中，都把贮氢材料作为重点研究领域之一。钢铁研究总院功能材料研究所近年来在国家“863”及国家自然科学基金多个项目的资助下，对各种贮氢材料开展了较深入的研究，取得了一些有特色的研究结果。为了加速我国贮氢材料的研究与产业化赶超世界先进水平以及加强与同行的交流，特整理出版了本书。

应用真空快淬技术制备贮氢合金是钢铁研究总院在贮氢材料研究中的一个特点，本书较全面地介绍了真空快淬工艺在稀土基 AB_5 型、Laves 相 AB_2 型、高容量 La-Mg-Ni 系 AB_3 型贮氢合金中的应用，较全面地总结了快淬态贮氢合金的微观结构及电化学性能特点。希望本书的出版对本领域从事研究工作的工程技术人员以及立志在本领域有建树的学者能起到抛砖引玉的作用。

本书遴选了自 2004 年以来在国际期刊上发表的与贮氢材料相关的部分研究论文，编入本书的论文全部被 SCI 收录。本书内容编排力求系统完整，

以便于读者对真空快淬技术在贮氢材料制备中的应用有一个较全面的了解。鉴于贮氢材料的发展日新月异，新材料、新技术、新成果浩瀚如烟，本书所涉及的内容仅可谓沧海一粟，挂一漏万。加之编者水平所限，本书内容，特别是英文写作方面存在的问题，恳请专家和读者不吝赐教。同时编者对本书收录的文章提出过宝贵意见的中外专家表示衷心的感谢。

编 者

2007年6月

PREFACE

Hydrogen is the most clean renewable energy with advantage of an inexhaustible supply. Oil-based modern energy system has pushed the world into the grip of severe energy crisis. Therefore, the research of non-carbon fuels is of great scientific value and social benefits. And humankind is looking forward to the exploitation and utilization of environment-friendly green energy. As one of the most important energy resources, hydrogen has attracted sufficient attention from different nations. The economical preparation, storage and transportation of hydrogen are the key subjects of hydrogen energy exploitation.

Because of their excellent ability of absorbing and desorbing hydrogen, hydrogen storage alloys now serve as important carriers in the storage and transportation of hydrogen. Moreover, as hydrogen and hydrogen storage alloys are both friendly to the environment, the international community is attaching great importance to them.

Metal hydride, carbon fiber, carbon nanotubes and certain kinds of organic liquids are good hydrogen storage materials. Especially, metal hydride is not only high quality hydrogen storage material, but also a new kind of functional material with broad application prospects, which can be applied in the transformation and storage of electric power, mechanical energy, heat energy and chemical energy. Therefore, metal hydride technology, including the research of materials and their applications, has enjoyed considerable worldwide attention and rapid development. China also attaches great importance to the research and development of hydrogen storage materials. In the "863" High-tech Development Plan, "973" Plan and the National Natural Science Foundation, hydrogen storage material is listed as a one of the key research areas. In recent years, the Division of Functional Materials of Central Iron & Steel Research Institute has carried out in-depth research in various hydrogen storage materials and achieved significant results, with the support of many foundations including national "863" Plan and the National Natural Science Foundation. The publication of the collected works is aimed at the acceleration of the research and industrialization of hydrogen storage materials in China to overtake the world's advanced level and the promotion of academic exchanges between experts in the area.

The application of rapid quenching technique in the preparation process of hydrogen storage alloys is a unique feature of the research of Central Iron & Steel Research Institute. The collected works provide readers with a comprehensive presentation of the application of vacuum rapid quenching process in rare earth based AB₅-type, Laves phase

AB₂-type, high-capacity La-Mg-Ni system AB₃-type hydrogen-storage alloys, and a comprehensive summary of microstructure and electrochemical properties of the rapid quenched hydrogen storage alloys. It is presented in hope of spurring more thorough research in the area.

It contains carefully chosen papers related to hydrogen storage alloys published in international journals since 2004, and all of the papers in this book were indexed by SCI. The editors tried their best to arrange the works in such a way that the readers can get a more comprehensive understanding of the application of vacuum rapid quenching technology in the preparation of hydrogen storage materials. However, in view of the rapid development and tremendous volume of scientific results of hydrogen storage materials, the book can be said to be a drop in the ocean and is far from complete. It is liable to mistakes or omissions, especially grammatical errors, so suggestions for improvement will be gratefully received. Any feedback offered, positive or negative, is welcomed with our sincere appreciation.

Editors

June, 2007

Contents

Microstructure and Electrochemical Characteristics of $\text{Mm}(\text{Ni}, \text{Co}, \text{Mn}, \text{Al})_5\text{B}_x (x=0\sim 0.4)$	
Hydrogen Storage Alloys Prepared by Cast and Rapid Quenching	1
Research of $\text{Mm}(\text{Ni}, \text{Mn}, \text{Al}, \text{Cu})_{4.9}\text{Co}_{0.2}$ Hydrogen Storage Alloys Prepared by Cast and Rapidly Quenched	8
Effect of Boron Additive on the Cycle Life of Low-Co AB_5 -type Electrode Consisting of Alloy Prepared by Cast and Rapid Quenching	14
The Effects of Rapid Quenching on the Electrochemical Characteristics and Microstructures of AB_2 Laves Phase Electrode Alloys	20
Effects of Rapid Quenching on the Electrochemical Performances and Microstructures of the $\text{Mm}(\text{Ni}, \text{Mn}, \text{Si}, \text{Al})_{4.3}\text{Co}_{0.6-x}\text{Fe}_x (x=0\sim 0.6)$ Electrode Alloys	26
Effect of Substituting Mn with La on the Electrochemical Performances of Co-free $\text{La}_x\text{Mm}_{1-x}(\text{Ni}, \text{Mn}, \text{Si}, \text{Al}, \text{Fe})_{4.9} (x=0\sim 1)$ Electrode Alloys Prepared by Casting and Rapid Quenching	33
Microstructures and Electrochemical Performances of $\text{La}_2\text{Mg}(\text{Ni}_{0.85}\text{Co}_{0.15})_9\text{Cr}_x (x=0\sim 0.2)$ Electrode Alloys Prepared by Casting and Rapid Quenching	40
Effect of Substituting Co with Fe on the Cycle Stabilities of the As-cast and Quenched AB_5 -type Hydrogen Storage Alloys	46
Effect of Rapid Quenching on the Microstructures and Electrochemical Performances of Co-free AB_5 -type Hydrogen Storage Alloys	52
Microstructures and Electrochemical Performances of $\text{La}_2\text{Mg}(\text{Ni}_{0.85}\text{Co}_{0.15})_9\text{M}_x (M=\text{B}, \text{Cr}, \text{Ti}; x=0, 0.1)$ Electrode Alloys Prepared by Casting and Rapid Quenching	58
Effect of Boron Additive on Electrochemical Cycling Life of La-Mg-Ni Alloys Prepared by Casting and Rapid Quenching	64
Electrochemical Characteristics of Mechanical Alloyed $(\text{Mg}_{1-x}\text{Zr}_x)_2\text{Ni} (x=0\sim 0.1)$ Electrode Alloys	69
Effects of Substituting Ni with Cu on the Microstructures and Electrochemical Characteristics of the As-cast and Quenched $\text{La}_{0.7}\text{Mg}_{0.3}\text{Ni}_{2.55-x}\text{Co}_{0.45}\text{Cu}_x (x=0\sim 0.4)$ Electrode Alloys	74
Research on Electrochemical Characteristics and Microstructure of $\text{Mm}(\text{Ni}, \text{Mn}, \text{Al})_{4.9}\text{Co}_{0.2}$ Rapidly Quenched Alloy	81
Research of Low-Co AB_5 Type Rare-earth-based Hydrogen Storage Alloy Electrodes	85
Electrochemical Characteristics and Microstructures of Rapidly Quenched $\text{Ti}_{0.5}\text{Zr}_{0.2}\text{Mn}_{0.2}\text{Cr}_{0.5}\text{V}_{0.2}\text{Ni}_{0.95}$ Alloy	90
Effect of Boron Addition on the Microstructures and Electrochemical Properties of $\text{MmNi}_{3.8}\text{Co}_{0.4}\text{Mn}_{0.6}\text{Al}_{0.2}$ Electrode Alloys Prepared by Casting and Rapid Quenching	95
The Effects of Rapid Quenching on the Microstructures and Electrochemical Properties of Low-Co AB_5 -type Electrode Alloy	101
Investigation on the Microstructure and Electrochemical Performances of $\text{La}_2\text{Mg}(\text{Ni}_{0.85}\text{Co}_{0.15})_9\text{B}_x (x=0\sim 0.2)$ Hydrogen Storage Electrode Alloys Prepared by Casting and Rapid Quenching	108
Effects of Substituting Co with Fe on the Microstructures and Electrochemical Characteristics of the As-cast and Quenched $\text{Mm}(\text{Ni}, \text{Mn}, \text{Si}, \text{Al})_{4.3}\text{Co}_{0.6-x}\text{Fe}_x (x=0\sim 0.6)$ Electrode Alloys	114
The Cycle Stabilities of the As-cast and Quenched $\text{La}_2\text{Mg}(\text{Ni}_{0.85}\text{Co}_{0.15})_9\text{M}_x (M=\text{B}, \text{Cr},$	

Ti; $x=0, 0.1$) Hydrogen Storage Alloys	122
Microstructure and Electrochemical Performances of $\text{La}_{0.7}\text{Mg}_{0.3}\text{Ni}_{2.55-x}\text{Co}_{0.45}\text{Cu}_x$ ($x=0\sim 0.4$)	
Hydrogen Storage Alloys Prepared by Casting and Rapid Quenching	128
Microstructure and Electrochemical Performances of $\text{La}_{0.7}\text{Mg}_{0.3}\text{Ni}_{2.55-x}\text{Co}_{0.45}\text{Al}_x$ ($x=0\sim 0.4$)	
Hydrogen Storage Alloys Prepared by Casting and Rapid Quenching	134
Effects of Cr Addition on the Microstructures and Electrochemical Properties of As-cast and	
Quenched $\text{La}_2\text{Mg}(\text{Ni}_{0.85}\text{Co}_{0.15})_9$ Electrode Alloys	141
Electrochemical Characteristics of $\text{Mg}_{2-x}\text{Zr}_x\text{Ni}$ ($x=0\sim 0.6$) Electrode Alloys Prepared by	
Mechanical Alloying	148
Investigation on Microstructures and Electrochemical Performances of the $\text{La}_{0.75}\text{Mg}_{0.25}\text{Ni}_{2.5}$	
Co_x ($x=0\sim 1.0$) Hydrogen Storage Alloys	154
Effects of Cr Addition on the Microstructures and Electrochemical Performances of La-Mg-Ni	
System(PuNi_3 -type) Hydrogen Storage Alloy	159
Investigation on the Microstructure and Electrochemical Performances of as-cast and Quenched	
$\text{La}_{0.7}\text{Mg}_{0.3}\text{Co}_{0.45}\text{Ni}_{2.55-x}\text{M}_x$ ($\text{M}=\text{Cu}, \text{Al}, \text{Mn}; x=0\sim 0.4$) Electrode Alloys	163
Cycle Stabilities of the $\text{La}_{0.7}\text{Mg}_{0.3}\text{Ni}_{2.55-x}\text{Co}_{0.45}\text{M}_x$ ($\text{M}=\text{Fe}, \text{Mn}, \text{Al}; x=0, 0.1$) Electrode	
Alloys Prepared by Casting and Rapid Quenching	168
Influences of the Substitution of Fe for Ni on Structures and Electrochemical Performances of	
the As-cast and Quenched $\text{La}_{0.7}\text{Mg}_{0.3}\text{Co}_{0.45}\text{Ni}_{2.55-x}\text{Fe}_x$ ($x=0\sim 0.4$) Electrode Alloys	174
Effect of Boron Addition on the Microstructure and Electrochemical Performances of	
$\text{La}_2\text{Mg}(\text{Ni}_{0.85}\text{Co}_{0.15})_9$ Hydrogen Storage Alloy	181
Microstructure and Electrochemical Performances of $\text{La}_{0.7}\text{Mg}_{0.3}\text{Ni}_{2.55-x}\text{Co}_{0.45}\text{M}_x$ ($\text{M}=\text{Cu}, \text{Cr},$	
$\text{Al}; x=0\sim 0.4$) Hydrogen Storage Alloys Prepared by Casting and Rapid Quenching	187
Effects of Substituting Ni with Al on the Microstructure and Electrochemical Performances of	
the as-cast and Quenched La-Mg-Ni-based(PuNi_3 -type) Hydrogen Storage Alloys	193
Effect of Substituting Ni with Cu on the Cycle Stability of $\text{La}_{0.7}\text{Mg}_{0.3}\text{Ni}_{2.55-x}\text{Co}_{0.45}$	
Cu_x ($x=0\sim 0.4$) Electrode Alloy Prepared by Casting and Rapid Quenching	199
Effect of Rapid Quenching on the Microstructures and Electrochemical Characteristics	
of $\text{La}_{0.7}\text{Mg}_{0.3}\text{Ni}_{2.55-x}\text{Co}_{0.45}\text{Al}_x$ ($x=0\sim 0.4$) Electrode Alloys	205
Effects of Substituting Mg with Zr on the Electrochemical Characteristics of Mg_2Ni -type	
Electrode Alloys Prepared by Mechanical Alloying	212
Effects of Rapid Quenching on Microstructures and Electrochemical Properties of $\text{La}_{0.7}$	
$\text{Mg}_{0.3}\text{Ni}_{2.55}\text{Co}_{0.45}\text{B}_x$ ($x=0\sim 0.2$) Hydrogen Storage Alloy	218
Investigation of Cobalt-free AB_5 -Type Hydrogen Storage Alloy	225
Effects of the Substitution of Al for Ni on the Structure and Electrochemical Performance of	
$\text{La}_{0.7}\text{Mg}_{0.3}\text{Ni}_{2.55-x}\text{Co}_{0.45}\text{Al}_x$ ($x=0\sim 0.4$) Electrode Alloys	228
Relations between Quenching Rate and Electrochemical Characteristics of $\text{Mm}(\text{Ni}, \text{Co}, \text{Mn}, \text{Al})_5\text{B}_x$	
($x=0\sim 0.2$) Electrode Alloys	234
The Effect of Rapid Quenching on the Microstructures and Electrochemical Performances	
of the $\text{La}_2\text{Mg}(\text{Ni}_{0.85}\text{Co}_{0.15})_9\text{M}_{0.1}$ ($\text{M}=\text{B}, \text{Cr}$) Hydrogen Storage Alloys	240
Effects of Substituting Ni with M ($\text{M}=\text{Cu}, \text{Al}$ and Mn) on Microstructures and	
Electrochemical Characteristics of La-Mg-Ni System(PuNi_3 -type) Electrode Alloys	246
Characterization of $\text{MmNi}_{3.6}\text{Co}_{0.75}\text{Mn}_{0.55}\text{Al}_{0.1}$ Alloys Prepared by Casting and Quenching	
Techniques	252
Electronic Structures of Hydrogen Storage Compounds, LaNi_5 and Its Micro-Hydrogenated	
Compounds	257

Microstructure and Electrochemical Characteristics of $\text{Mm}(\text{Ni}, \text{Co}, \text{Mn}, \text{Al})_5\text{B}_x$ ($x=0\sim 0.4$) Hydrogen Storage Alloys Prepared by Cast and Rapid Quenching

Zhang Yanghuan^{1,2}, Chen Meiyan², Wang Xinlin¹,
Wang Guoqing², Dong Xiaoping², Qi Yan¹

(1. Department of Functional Material Research, Central Iron and Steel Research Institute, Beijing, China;
2. Department of Material Science and Engineering, Baotou Iron and Steel University of Technology, Baotou, China)

ABSTRACT: Low Co AB_5 -type $\text{MmNi}_{3.8}\text{Co}_{0.4}\text{Mn}_{0.6}\text{Al}_{0.2}\text{B}_x$ ($x=0, 0.1, 0.2, 0.3, 0.4$) hydrogen storage alloys were prepared by cast and rapid quenching. The microstructures and electrochemical performances of the as-cast and quenched alloys were analysed and measured. The effects of boron additive and rapid quenching technique on the microstructures and electrochemical properties of as-cast and quenched alloys were investigated comprehensively. The experimental results showed that the microstructure of as-cast $\text{MmNi}_{3.8}\text{Co}_{0.4}\text{Mn}_{0.6}\text{Al}_{0.2}\text{B}_x$ ($x=0, 0.1, 0.2, 0.3, 0.4$) alloys was composed of CaCu_5 -type main phase and a small amount of CeCo_4 B-type secondary phase. The abundance of the secondary phase increases with the increase of boron content x . The rapid quenching techniques were used in the preparation of the alloys. The amount of secondary phase in the alloys decreased with the increase of quenching rate. Rapid quenching made lattice constants increase slightly. The effects of rapid quenching on the electrochemical performances of the alloys are very significant. The discharge capacity of the alloys decreased obviously and the cycle stability increased dramatically with the increase of quenching rate. Rapid quenching made the activation capability of the alloys lowered. However, the activate performance and high rate discharge capability as well as discharge voltage characteristic of the alloys were modified obviously with the increase of boron content x .

KEYWORDS: hydrogen storage alloy; boron additive; rapid quenching; microstructure; electrochemical characteristic

1 INTRODUCTION

AB_5 -type (Original LaNi_5) hydrogen storage alloy is being used widely because it can reversibly absorb and release hydrogen at room temperature and can be easily activated as well as produce high reaction rate of absorbing and releasing hydrogen. Although AB_5 -type hydrogen storage alloy has been industrialized in large-scale in some countries, especially in America, Japan and China, the investigation on the AB_5 -type hydrogen storage alloy has been carrying out in order to improve the electrochemical characteristics and reduce the production cost of the alloy^[1,2]. The majority of the papers published by International Symposium on Metal Hydrogen System-Fundamental and Application, Annecy, France, September 2002 still concentrated on the investigation of AB_5 -type hydrogen storage alloy.

The decrease of Co content in alloy is very beneficial to reduce the production cost of the alloy, whereas the function of Co on the cycle life of the AB_5 -type hydrogen storage alloy is extremely important^[3]. Therefore, the investigation focus on AB_5 -type hydrogen storage alloy is how to enhance the cycle stability of low-Co electrode alloy.

It is very difficult to enhance the cycle stability of low-Co AB_5 -type hydrogen storage alloy by traditional cast technique. Literature^[4] reported that the low-Co AB_5 -type hydrogen storage alloy with special microstructure, which is composed of microcrystal, nanocrystal and amorphous phase, could be prepared by composition adjusting and rapid quenching. The alloy thus prepared has excellent activation

performance and cycle stability. In order to modify the cycle life of low-Co AB_5 -type hydrogen storage alloy, a trace of boron was added and rapid quenching techniques were used in the preparation of the alloys. The obtained results indicated that boron additive could enhance the cycle life of as-cast AB_5 -type hydrogen storage alloy, and rapid quenching treatment made the function of boron on the cycle life more significant.

The paper mainly discussed the microcosmic mechanism of the influences of boron additive and rapid quenching technique on the electrochemical characteristics of low-Co AB_5 -type hydrogen storage alloy.

2 EXPERIMENTAL DETAILS

2.1 Preparation of Alloys

The experimental alloys were melted by induction furnace under an argon atmosphere. The melt was poured into a copper mould cooled by water, and a cast alloy ingot was obtained. Part of the as-cast alloys was re-melted and quenched by melt-spinning with a rotating copper wheel, obtaining flakes of the as-quenched alloy with quenching rates of 22, 30 and 38 m/s. The quenching rate was expressed by the linear velocity of the copper wheel. The chemical composition of the experimental alloy was $\text{MmNi}_{3.8}\text{Co}_{0.4}\text{Mn}_{0.6}\text{Al}_{0.2}\text{B}_x$ ($x=0, 0.1, 0.2, 0.3, 0.4$). The alloys, which correspond with boron content x , were represented by B_0 , B_1 , B_2 , B_3 and B_4 , respectively. The purity of all the component metals (Ni, Co, Mn, Al) is at least 99.8%. The

purity of boron is 99.93%, Mm denoted Ce-rich mischmetal ($w(\text{La})=23.70\%$, $w(\text{Ce})=55.29\%$, $w(\text{Pr})=5.28\%$, $w(\text{Nd})15.70\%$), and the purity is 99.85%.

2.2 Electrode Preparation and Electrochemical Measurement

The fractions of the as-cast and quenched alloys, which were ground mechanically into powder below 200 meshes, were used for the preparation of experimental electrode. The electrode pellets with 15 mm in diameter were prepared by mixing 1 g alloy powder with fine nickel powder in a weight ratio of 1 : 1 together with a small amount of polyvinyl alcohol (PVA) solution as binder, and then compressed under a pressure of 35 MPa. After drying for 4 h, the electrode pellets were immersed in 6mol/L KOH solution for at least 24 h in order to wet fully the electrode before the electrochemical measurement. The pellet was tightly wrapped with foam nickel slice and was bound with nickel wire. Thus an experimental electrode was prepared. In order to avoid the influence of the difference of the preparation methods on the electrochemical properties of the experimental electrodes, all of the electrode pellets were prepared by exactly same method so that it can be ensured that the electrochemical properties of the electrodes only depend on the characteristics of the alloys.

The electrochemical properties of the experimental electrodes were tested in a tri-electrode open cell, which consists of a working electrode (metal hydride electrode), a counter electrode ($\text{NiOOH}/\text{Ni}(\text{OH})_2$) and a reference electrode (Hg/HgO). The electrolyte was a 6mol/L KOH solution. The voltage between the negative electrode and the reference electrode was defined as the discharge voltage. Every cycle was overcharge to about 50%, with constant current, resting 15 min and -0.500 V cut-off voltage. The environment temperature of measurement was kept at 30°C . The activation performance and the maximum discharge capacity were measured with a current density of 60 mA/g, and the cycle life was measured with a current density of 300 mA/g.

2.3 Microstructure Determination and Morphology Observation

The sample of the as-cast alloys were directly polished, and flakes of the as-quenched alloys were inlaid in epoxy resin for being polished. The samples thus prepared were etched with a 60% hydrofluoric acid. The morphologies of as-cast and quenched alloy were observed by SEM and optical microscope. The samples of the as-cast and quenched alloys were pulverized by mechanical grinding, and the size of the powder samples was less than $70\text{ }\mu\text{m}$. The phase structures of the alloys were detected by XRD, and the type of X-ray diffractometer used in this experiment was $D/\text{max}/2400$. The diffraction was performed with $\text{Cu K}\alpha_1$ and the rays were filtered by graphite. The experimental parameters for determining the phase structure were 160 mA, 40 kV and $10^\circ/\text{min}$. The lattice constants were measured by step scanning, and the experimental parameters were 160 mA, 50 kV and 0.02° per step and 1 per step equivalent to $1.2^\circ/\text{min}$. The powder samples were dispersed in absolute alcohol for observing grain morphology with TEM, and for determining with selected area electron diffraction (SAD) whether an

amorphous phase existed in the samples.

3 RESULTS AND DISCUSSION

3.1 Electrochemical Characteristics of the Alloys

3.1.1 The Activation Capability of the Alloys

Activation number denoted by n was characterized by the number of charge-discharge cycle required for attaining the maximum discharge capacity through a charge-discharge cycle at the constant current density of 60 mA/g. Fig. 1 illustrated the cycle number dependence of the discharge capacity of the alloys prepared by cast and rapid quenching (30 m/s), respectively, and the discharge current density was 60 mA/g. It could be derived from Fig. 1 that all of the as-cast and quenched alloys could be activated easily. The cast alloys could be completely activated after two to four cycles, and it needed two to six cycles for the quenched alloys. The addition of boron modified the activation performance of the as-cast alloys and made the activation performance of the as-quenched alloys decreased slightly. Obviously, the activation performance of the alloys is intimately relevant with the phase structure, surface characteristic, grain size and interstitial dimension of the alloys^[5].

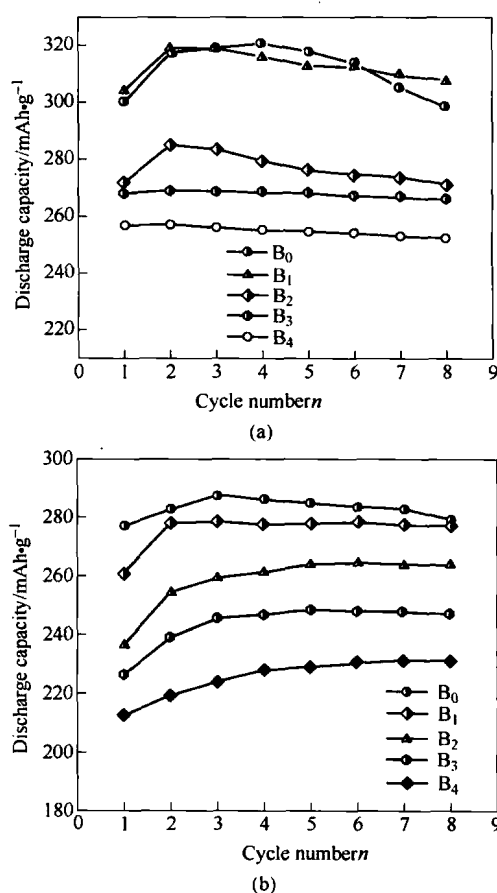


Fig. 1 The relationship between the cycle number and the discharge capacity of the as-cast ;(a) and as-quenched (b) alloys

3.1.2 The Discharge Capacity and the High Rate Discharge Capability of the Alloys

Boron content x and quenching rate dependence of the maximum discharge capacity was illustrated in Fig. 2. It

could be seen from Fig. 2 that the maximum discharge capacities of the as-cast and quenched alloys decreased with the increase of boron content x , when boron content x increased from 0 to 0.4, the maximum discharge capacities of the as-cast alloys were reduced from 320 to 257 mAh/g; for as-quenched alloys obtained with quenched rate of 22 m/s, from 300 to 240 mAh/g. The effect of rapid quenching on the discharge capacity of the alloys was significant. The discharge capacity of the experimental alloys decreased with the increase of quenching rate. When quenching rate increased from 0 m/s (As-cast was defined as quenching rate of 0 m/s) to 38 m/s, the maximum discharge capacity of B₄ alloy was reduced from 257.2 to 231.5 mAh/g.

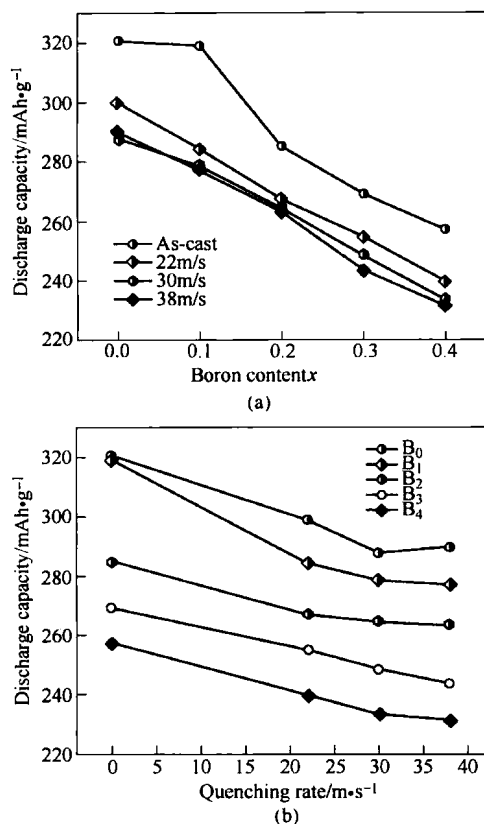


Fig. 2 Boron content (a) and quenching rate (b) dependence of the maximum discharge capacity of as-cast and quenched alloys

$C_{60\max}$ and $C_{300\max}$ (in mAh/g units) represented the maximum discharge capacities with charge-discharge current densities of 60 and 300 mA/g, respectively. C_h represented 1C rate discharge capability, $C_h = C_{300\max}/C_{60\max} \times 100\%$. Boron content and quenching rate dependence of the 1C rate discharge capability were illustrated in Fig. 3. It could be seen from Fig. 3 that 1C rate discharge capability of the as-cast and quenched alloys increased with the increase of boron content x . When boron content x increased from 0 to 0.4, 1C rate discharge capability of as-cast alloys was enhanced from 89.02% to 93.61%; for as-quenched alloys with quenching rate of 38 m/s, from 77.62% to 89.82%. Obviously, the effect of boron on rate discharge capability of the as-quenched alloys was more significant than on that of the as-cast alloy. Quenching rate had an obvious influence on the rate discharge capability of the alloys. The rate dis-

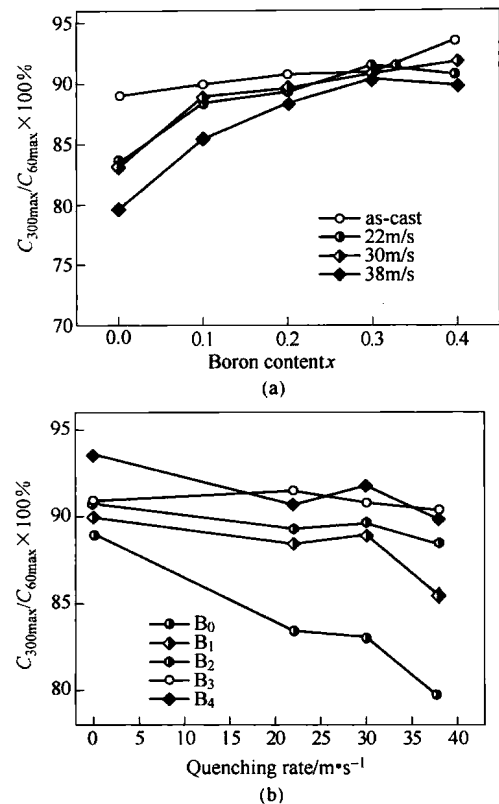


Fig. 3 Boron content x (a) and quenching rate (b) dependence of the 1C rate discharge capability

charge capability of the alloys decreased with increase of quenching rate. It was worthy of attention that the effect of quenching rate on the rate discharge capability of the alloys decreased with the increase of boron content x . The high rate discharge capability of hydrogen storage alloy is a dynamic problem. Generally, the discharge of hydrogen storage alloy includes three processes^[6,7]: (1) Electrochemical reaction; (2) Hydrogen diffusion; (3) $\alpha \rightleftharpoons \beta$ phase transformation. According to aforementioned three essential processes, we could conclude that high rate discharge of the alloys must meet two conditions: (1) The diffusion rate of hydrogen atom in the alloy must be fast enough. (2) The electric catalytic activation of alloy surface must be large enough.

3.1.3 The Discharge Voltage Characteristics of the Alloys

In order to compare the characteristics of the discharge voltage plateaus, the discharge voltage curves of the alloys with different compositions and quenching rate were put in a figure (Fig. 4). The longer and even the discharge volt age plateau, the better the discharge voltage characteristic. In addition, the discharge plateau voltage is an important property. It could be found visibly from Fig. 4a that the addition of boron modified significantly the discharge voltage characteristics of the as-cast alloys, elevated the discharge plateau voltage, and decreased the slope of the discharge voltage plateau. Rapid quenching made the discharge plateau voltage decreased, and its effect on the slope of discharge voltage plateau was not obvious.

3.1.4 The Cycle Lives of the Alloys

Cycle life indicated by N was characterized by the cycle number after which discharge capacity of the alloy with the current density of 300 mA/g was reduced to 60% of the

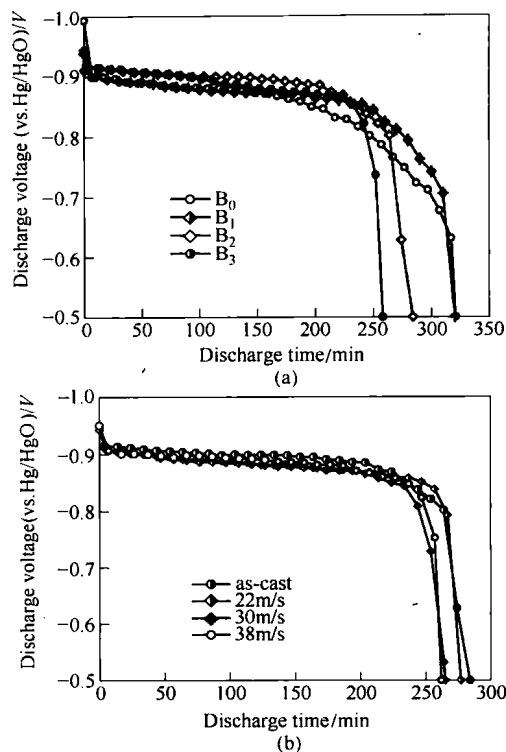


Fig. 4 The influences of boron content (a) and quenching rate (b) on the discharge voltage

maximum capacity. Fig. 5 illustrated the cycle number dependence of the discharge capacity of the alloys prepared by

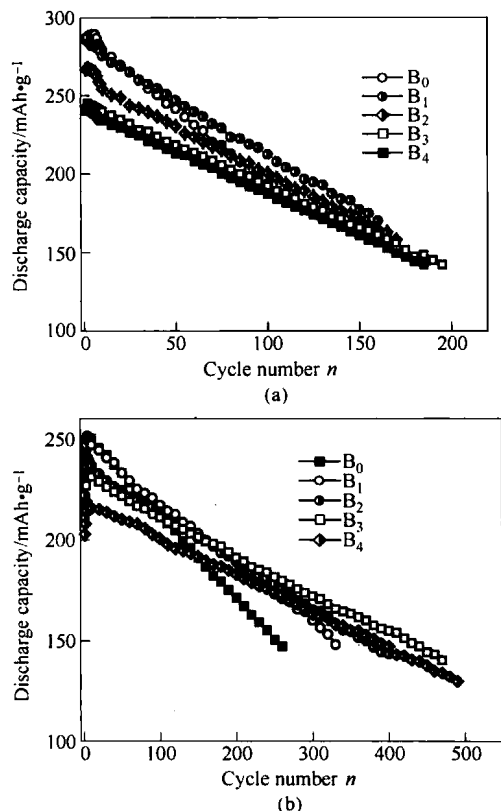


Fig. 5 The relationship between the cycle number and the discharge capacity of as-cast (a) and as-quenched; (b) alloys

cast and rapidly quenched (22 m/s), respectively. It can be derived from Fig. 5 that the slopes of curves corresponding with as-cast and quenched alloys decreased with the increase of boron content x . It indicated that the addition of boron was advantageous to the cycle lives of the alloys. In order to show clearly the effects of boron and quenching rate on the cycle lives of the alloys, the boron content x and quenching rate dependence of the cycle lives of the alloys were illustrated in Fig. 6. It could be seen from Fig. 6 that cycle lives of the as-cast and quenched alloys significantly increased with increase of boron content x . When boron content x increased from 0 to 0.4, the cycle life of the as-cast alloy was enhanced from 118 to 183 cycles, and for as-quenched (38 m/s) alloy, from 310 to 566 cycles. Obviously, the effect of boron on the cycle life of the as-quenched alloy is more significant than on that of the as-cast alloy. The cycle life of the as-quenched alloy is longer than that of the as-cast alloy, and the cycle life of as-quenched alloy increased remarkably with the increase of quenching rate (Fig. 6b). It indicated the cycle stability of hydrogen storage alloy is intimately relevant to the composition of the alloy and its preparation technique.

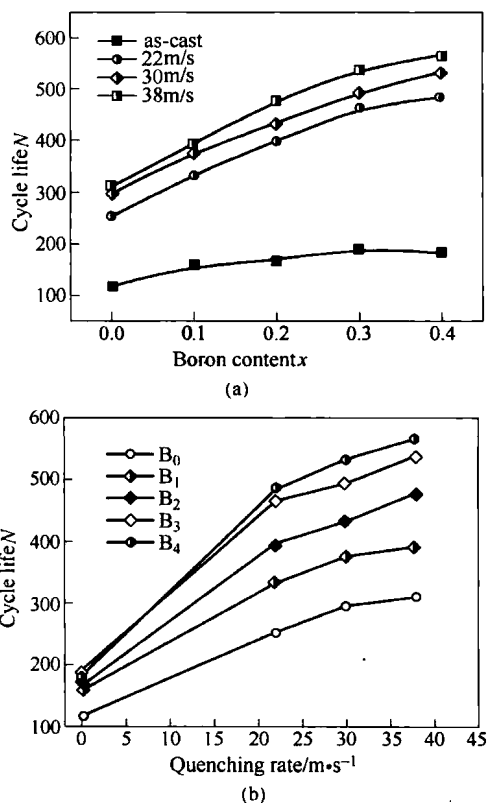


Fig. 6 Boron content x (a) and quenching rate (b) dependence of the cycle lives of the alloys

3. 2 Determination and Observation of Microstructure

3. 2. 1 The Determination of the Phase Structure of the Alloy

The phase structures of the as-cast and quenched alloys were determined by XRD. The X-ray diffraction diagrams of the as-cast and quenched alloys were illustrated in Fig. 7. It could be derived from Fig. 7 that as-cast alloy without boron

(B₀) has a single phase structure with CaCu₅-type. However, all of the as-cast alloys with boron (B₁~B₄) have a two-phase structure that is composed of a CaCu₅-type main phase and a

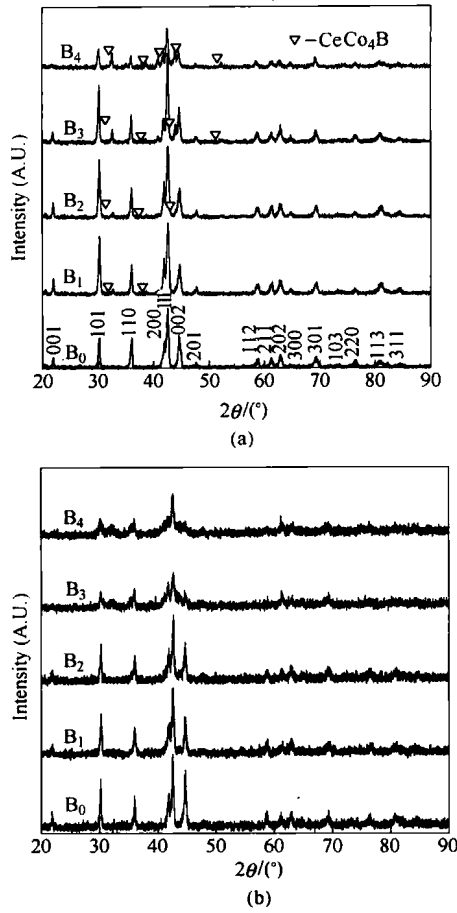


Fig. 7 The X-ray diffraction diagrams of the as-cast(a) and as-quenched (b) alloy

small amount of CeCo₄ B-type secondary phase. Both main phase and secondary phase belong to hexagonal system with P6/mmm space group. The abundance of the CeCo₄ B-type secondary phase increased with the increase of boron content x . All of the as-quenched alloys (B₀~B₄) obtained with quenching rate of 22 m/s have a single phase structure with CaCu₅-type, and CeCo₄ B-type secondary phase disappeared nearly. The lattice constants of the as-cast and quenched alloys obtained with quenching rate of 22 m/s, which were calculated from the diffraction peaks of (1 0 1), (1 1 0), (2 0 0), (1 1 1) and (0 0 2) crystal planes of the main phase of the alloys by a method of least squares, were listed in Table 1. It could be derived from Table 1 that the addition of boron had a slight influence on the lattice constants of the main phase. The c axis of the main phase of the as-cast alloys slightly increased with the increase of boron content x , whereas a -axis of the main phase decreased imperceptibly. It is reasonable to roughly quantify the amount of the secondary phase of the as-cast alloys by using the relative integral intensity of the strongest peak (1 1 1) for CaCu₅-type phase and the strongest peak (1 1 2) for CeCo₄ B-type phase because the main phase and the secondary phase belong to the same space group. The ratio of integral intensity of the peak

(1 1 2) for CeCo₄ B-type phase vs. the total integral intensity of the peak (1 1 1) for CaCu₅-type phase and the peak (1 1 2) peak for CeCo₄ B-type phase was calculated as the abundance of the secondary phase of the as-cast alloys (B₁~B₄), and the calculated results were also listed in Table 1. It could be derived from Table 1 that the abundance of the secondary phase in the as-cast alloys with boron (B₁~B₄) increased with the increase of boron content x . When boron content x increased from 0.1 to 0.4, the amount of the secondary phase increased from 3.21% to 20.26%.

The reason of the addition of boron modifying the activation capability of the as-cast alloy is attributed to the formation of the secondary phase. The formation of the secondary phase increases the number of phase boundaries, which provide extra tunnels for the diffusion of hydrogen atoms and probably is buffer area of the releasing of the stress formed in the process of hydrogen absorbed. The effects of boron addition on the activation capability of as-quenched alloys were complicated; the addition of boron increasing the diffusion coefficient of hydrogen atom in the alloy is favourable for the activation capability^[9], and boron strongly promoting the formation of amorphous phase is unfavourable. Therefore, whether boron addition would increase or decrease the activation capability of the as-quenched alloy depended on the predominant one of the above. Author considered that the effect of amorphous was much stronger. Therefore, the activation performance of the as-quenched alloys decreased slightly with the increase of boron content.

The discharge capacity of the as-cast alloys lowered remarkably with the increase of boron content x . It was directly relevant to the formation of the secondary phase in the alloys. Because CeCo₄ B-type secondary phase is a non-hydride phase, so, the larger the amount of secondary phase, the lower the discharge capacity of the alloys. In addition, rapid quenching made the lattice constants and cell volume of the alloys increased, and it is advantageous to the modification of the cycle stability and the increase of the discharge capacity of the alloys.

The cycle stability of hydrogen storage alloy is a decisive factor of the life of Ni-MH battery. The root cause of leading to battery lose efficacy is on negative electrode, rather than on positive electrode. The failure of battery is characterized by the decay of the discharge capacity and the decrease of the discharge voltage. The literatures^[3,8] confirmed that the fundamental reason for the capacity decay of hydrogen storage alloy is the pulverization and oxidation of the alloy in process of the charge-discharge cycle. The lattice internal stress and cell volume expansion, which are inevitable when hydrogen atoms enter into the interstitials of the lattice, are real driving force, which leads to the pulverization of the alloy. The reason for the addition of boron enhancing the cycle life of the as-cast alloy was attributed to the formation of the secondary phase. The formation of the secondary phase increased the amount of phase boundary, which probably is a buffer area of the releasing of the stress formed in the process of hydrogen absorbing. Therefore, the anti-pulverization property of the as-cast alloys was improved significantly. However, the cycle lives of the alloys with boron were enhanced dramatically by rapid quenching. Obviously, it has no relation with the secondary phase, and

Table 1 Cell parameter and volume of CaCu_5 -type main phase; the abundance of secondary phase in the as-cast alloys with boron

Sample	Lattice constant				Cell volume/ V (\AA^3)		abundance of secondary phase/%	
	$a/\text{\AA}$		$c/\text{\AA}$		as-cast	22 m/s	as-cast	22 m/s
	as-cast	22m/s	as-cast	22m/s				
B_0	5.017	5.021	4.051	4.053	88.31	88.49	—	—
B_1	5.016	5.023	4.053	4.054	88.32	88.58	3.21	—
B_2	5.016	5.022	4.059	4.062	88.45	88.72	3.88	—
B_3	5.015	5.024	4.061	4.062	88.45	88.78	14.48	—
B_4	5.014	5.023	4.061	4.063	88.42	88.78	20.26	—

differences of the cycle lives of the alloys with boron ($B_1 \sim B_4$) were very large although the same rapid quenching technique was used. So, it is very necessary to further investigate on the microstructures of the alloys in order to explain the mechanism of the change in the cycle life.

3.2.2 The Observation of the Microstructure and Morphology of the Alloy

Literature^[10] investigated the hydrogen absorbing capability of La-Ni alloy amorphous film, and the results showed that the capacity of the amorphous film was half as large as that of the crystal alloy. Therefore, it seems that the main reason of rapid quenching leading to the decrease of the capacity of the alloy probably was because of the formation of amorphous phase. Thus, the crystalline state of the as-quenched alloys was determined by TEM, and the results were illustrated in Fig. 8. It could be seen from Fig. 8 that amorphous phase formed in the alloys (B_0 and B_4) obtained

with quenching rate of 22 m/s, and the amount of the amorphous phase in B_0 alloy was much less than that in B_4 alloy. The complete crystal morphology of B_0 alloy could be seen clearly, whereas we could not see it in B_4 alloy. It could be seen from Fig. 7(b) that the X-ray diffraction peak of the as-quenched B_4 alloy (22 m/s) widen and its height lowered significantly. It indicated the existence of amorphous phase in the alloy. The amount of amorphous phase in B_0 and B_4 alloys prepared by same rapid quenching technique was different. Obviously, it should be mainly ascribed to the function of boron additive. The experimental results indicated that the amount of amorphous phase increased with the increase of quenching rate. Therefore, it could be conclude that the great difference of the electrochemical performance of the as-quenched alloys with different boron contents was attributed to the difference of the amounts of amorphous phase in the alloys. The influences of rapid quenching on the capacity are

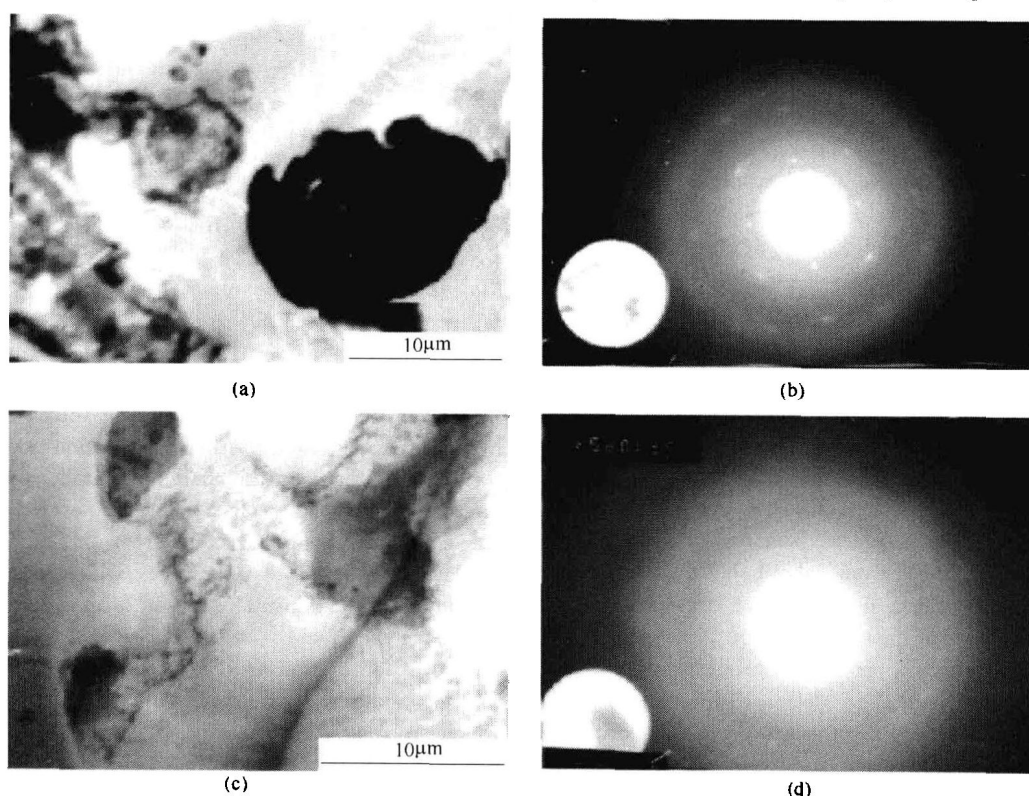


Fig. 8 The morphologies (a, c) and SAD (b, d) of the as-quenched B_0 and B_4 alloys (22 m/s) (TEM)